

## Speckle Interferometric Observations on 2.6 m telescope of BAO

J.A.Docobo<sup>1</sup>, J. Gomez<sup>1</sup>, N.D.Melikian<sup>2</sup>, G.Paronyan<sup>2</sup>

<sup>1</sup>*Astronomical Observatory Ramon Maria Aller of the University of Santiago de Compostela, Spain*

<sup>2</sup>*NAS RA V. Ambartsumian Byurakan Astrophysical Observatory (BAO), Armenia*

### Abstract

Speckle observations with a Photon Max EMCCD detector from Princeton Instruments were carried out for the first time in the 2.6 m telescope of BAO. Three observing campaigns were already completed. More than four hundred objects had been observed, relative positions and differential photometry information will be published during next months. Throughout the text we provide general information regarding the campaigns, the camera configuration, the EMCCD technical characteristics, and the reduction procedure. Also a brief discussion on how to determine the angle without the 180° ambiguity is included .

### 1. Introduction

Speckle observations of binary stars contribute to obtain thousands of new measurements every year (Horch et al. 2017, Tokovinin et al. 2016). The monitoring of these systems remains as an important tool to understand stellar structure and evolution, as they provide empirically-determined masses. Also generously sized samples of orbital information and differences of the magnitudes can be used to explore the role that stars play in formation mechanisms, and the difference between single and multiple scenarios. In addition, speckle interferometry allows to observe even when the conditions are far from being ideal, from the photometrical point of view, and the acquisition times lie in the range of a couple of minutes. The use of electron-multiplying CCDs (EMCCDs) has increased the capabilities and the quality of the data recorded in the last decade. The new possibilities that these cameras provided, together with their market value, turn them into an excellent tool to conduct observations using different techniques not only speckle interferometry, but also lucky imaging or lunar occultations.

J.A. Docobo, Director of the Astronomical Observatory Ramón María Aller of the University of Santiago de Compostela (OARMA, Galicia, Spain) and H.A.Harutyunyan, Director of the Byurakan Astrophysical Observatory (BAO, Armenia) signed an agreement in January 2010 to allow that the OARMA sent its own EMCCD speckle interferometry camera to BAO with the aim to attach it to the 2.6 m telescope of BAO. The objective of the agreement is to obtain data that could be

used for astrometric and astrophysical investigations of single and multiple objects in stellar aggregates, associations and within Solar vicinity. Technical complications and maintenance work in the telescope, including mirror aluminized, delay the use of the camera several years.

Recently, speckle observations were carried out for the first time in the 2.6 m telescope of BAO. We observed during five nights in October 2016, eight nights between May and Jun 2017, plus ten nights in October and November 2017. General information regarding each campaign can be found in Table 1.

**Table 1.** *Campaigns Resume*

<b>Campaign</b>	<b>Nights</b>	<b>Objects</b>	<b>Science Blocks</b>	<b>Dark Blocks</b>	<b>Flat Blocks</b>	<b>Wide Field Blocks</b>
Oct 2016	5	67	228	15	0	4
May Jun 2017	8	183	429	24	14	11
Oct Nov 2017	10	183	435	65	48	19

## 2. Description of the camera

We used a camera that merge a speckle oriented optical configuration together with a Photon Max EMCCD detector from Princeton Instruments. The detector utilizes a  $512 \times 512$  pixel, back-illuminated EMCCD with  $>90\%$  quantum efficiency and  $< 1 e^-$  rms read noise, allowing single photon sensitivity with sufficient multiplication gain. Deep thermoelectric cooling down to  $-70^\circ C$  reduces the dark current below  $0.01 e^-s^{-1}$  per pixel. The detector has a pixel size of  $16 \times 16 \mu m$ , and an imaging area of  $8.2 \times 8.2 mm^2$  is covered. It corresponds to the angular field of view of  $168''.7$  in the prime focus of the 2.6 m telescope ( $F/3.85$ , scale  $20''.6 mm^{-1}$ ) and a resolution of  $0''.33$  pixel $^{-1}$ . With 8x and 20x objective microscopes, angular fields of  $21''.1$  and  $8''.4$  are covered, respectively. The system is capable of acquiring and storing 16 bit digitized data at a frame rate of up to 20 fps at full resolution, with  $\sim 38$  ms readout time per frame. Single photoelectron events are recorded with a signal-to-noise ratio of about 50. Details regarding previous observations with this camera can be found in (Tamazian et al. 2008, Docobo et al. 2010).

The preliminary estimations are show that under good seeing conditions, binary components as faint as 12 mag in optical wavelengths are observed. The diffraction-limited resolution in the optical wavelengths is below 90 mas. Filters with the centre wavelength/ bandwidth of 550/20 nm, 600/40 nm, 650/40nm, 700/80nm and 800/100 nm were used. Additional information regarding the EMCCD, the filters

characteristics, and the Risley prisms for Atmospheric Dispersion Correction can be found in (Maksimov et al. 2009).

We used the 10Mhz frequency operating readout in Frame Transfer mode and the Low Light option was selected in the controller gain. It sets the relation between the electrons acquired in the CCD and the ADUs generated. The highest multiplication gain value, 4095, were used to most, except for a few bright objects. It implies a multiplication gain factor in excess of 1000x. Before each exposure the CCD is cleaned two times. No flip or rotation had being apply to the images. According to our installation the south is in the top of the frame, the north in the bottom and west/east in the left/right sides. More information regarding all the possibilities that the PhotonMax offers in both, standard application as normal CCD and high speed low light level multiplication gain mode can be found in its manual.

### **3. Observing procedure**

In preparation for the observing campaigns, we tested the components and the installation procedure during May/June 2016. The camera observed his first light in BAO at Oct 12, 2016, when we checked if all the components were working properly. Another tests, mainly related with the behaviour of the camera under usual and non-usual settings (binning, operating readout frequency of 5Mhz, light mode, etc.) had being carried during moments where the observations were not feasible because of the weather.

The observing program selection and the efficiency on the part of the telescope operators are the base of an optimal use of the allocated telescope time. In average, we were able to observe about four stars per hour, dedicating ten minutes to selection the desired object and guiding the telescope, as well as five minutes to data acquisition and recording. In general two data cubes are obtained per object. More than two blocks were recorded in the case of high priority systems, but also for those triple systems with separation between components bigger than the field of view provided by the 20x microscope objective. Each data cube contains 1000 images of 512 x 512 format, with 16 bits per pixel. Few objects had being observed in more than one campaign at the moment.

Most often, at the beginning of each night of observations, a reference star is observed. Usually a close to zenith bright single object selected by the telescope operator. For direct calibration of the camera scale and orientation angle we have observed speckle interferometric binaries with orbits graded 1 or 2 taken from the updated version of the Sixth Catalogue of Orbits of Visual Binary Stars (Hartkopf et al.

2001). We also obtained images from open systems with the aim to do an independent calibration.

The camera creates a SPE archive per observation into the camera operator's computer memory. As the software was not interfaced neither to the telescope guiding software nor to the camera optical settings, which include filters, prism and microscopes configuration, all this information must be incorporated by hand to our logbook. Using it, plus the original SPE files, we generate the final FITS blocks. Most of the relative positions and magnitude differences of each binary are derived after the end of the campaign. Object identification must be checked *post factum* and corrected in the few cases that we did not point to the correct component of the system observed.

#### 4. Reduction procedure

To calculate the relative positions, we use the ensemble-averaged power spectrum (PS) of speckle interferograms without compensation for the atmospheric transfer function. If we denote as  $\nu$  a spatial frequency vector, the Fourier transform of the object intensity distribution as  $O(\nu)$ ,  $\langle |S(\nu)|^2 \rangle$  being the speckle interferometric transfer function (STF) and  $N(\nu)$  representing the power spectrum of noisy events, then the power spectrum of an image cube, that is calculated by summing the square modulus of the Fourier Transform of each image, must verify,

$$\langle |I(\nu)|^2 \rangle = |O(\nu)|^2 \langle |S(\nu)|^2 \rangle + N(\nu)$$

Pluzhnik (Pluzhnik et al. 2005) described how  $N(\nu)$  is mainly determined by read-out noise and photon noise, where the second one is much larger in modern detectors. Meanwhile, as can be observed in Figure 1, our camera shows a slightly increase in the mean intensity of the dark frame until it reaches a stable value after 350-400 images. To correct this effect we obtain the frame-to-frame average of different dark blocks to create a "super-block" and subtract frame by frame our science images minus the correspondent dark one. In order As these images share the same position within the block, the read-out effect from "super-dark" and science observations should be similar. We found this method to be more reliable concerning to our camera characteristics than just subtract the average dark frame of a single block. Considering now the photon bias influence, the aforementioned author decompose it as  $N_p(\nu) = N_0 n_p(\nu)$ , where  $N_0$  reflects the photon bias amplitude and the other term is defined as the normalized photon bias term. The normalized

photon bias is linked with the photon bias shape, and it can be removed dividing the power spectrum by the normalized power spectrum of a flat field block obtained with the same configuration as the science block. The difference between both power spectrums calculated with and without corrections can be appreciated comparing them in Figure 2.

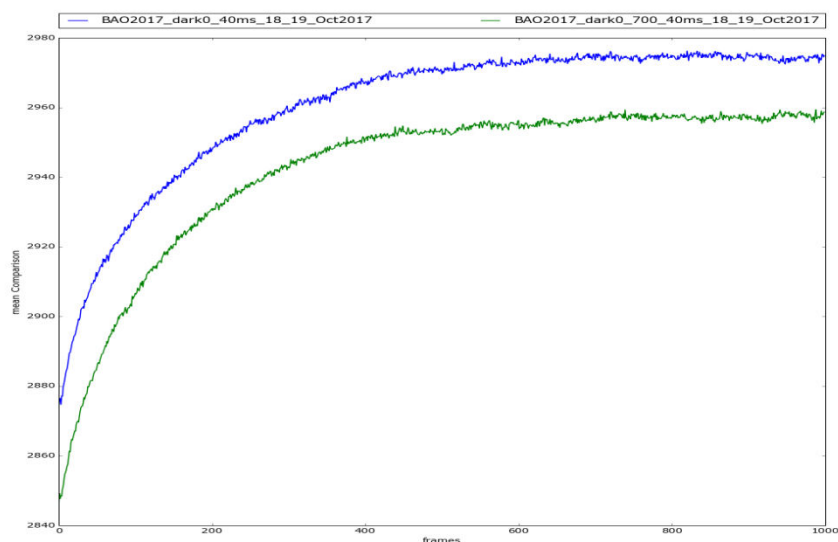


**Figure 1.** Comparative between two darks

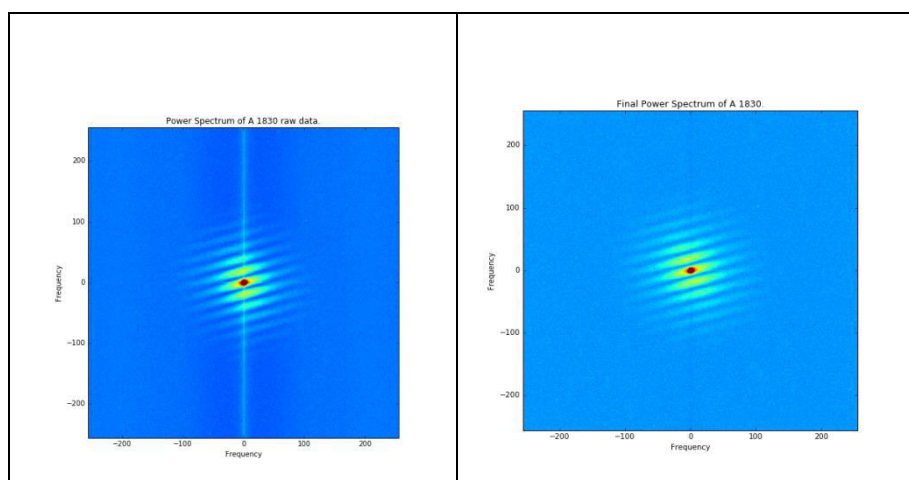


**Figure 2.** Power spectra of A1830 without any kind of correction (left) and after subtract superdark image by image and correct by flat power spectrum (right).

Whereas, the photon bias amplitude  $N_0$  can be obtained averaging the power spectrum beyond the cutoff frequency of the telescope where  $|O(\nu)|^2 < |S(\nu)|^2 >$  must be equal to zero. The mean of this outer region is subtracted from the power spectrum. After performing these corrections, we mask the central peak plus the central column and row (see Fig. 3).

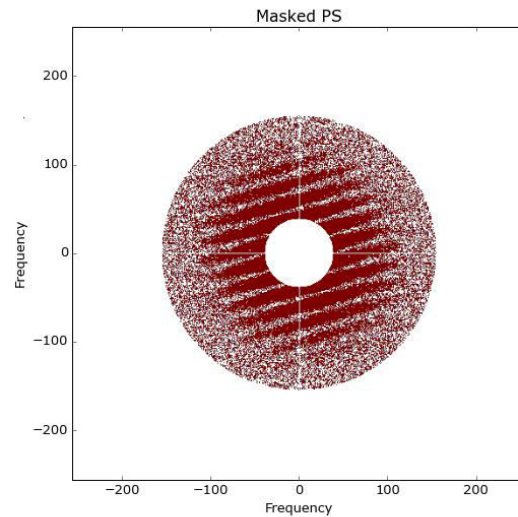


**Figure 3.** Masked image of the previous spectrum. The cutoff frequency is determined by the diameter of the telescope, the filter used for the observation and the pixel size. The central mask is 10% of the cutoff value in this example. We also masked central row and column.

Finally, we calculate its autocorrelation function (ACF), using the image generated to detect the secondary peak position. Nevertheless, the ACF duplicates the information generating a “phantom” peak symmetrical to the real one, as it can be seen in Figure 4. At this point we have just determined the angle with an uncertainty of  $180^\circ$ . In some cases past observations can appoint which is the real and the phantom peak. In other cases, the absolute quadrant determination problem arises.

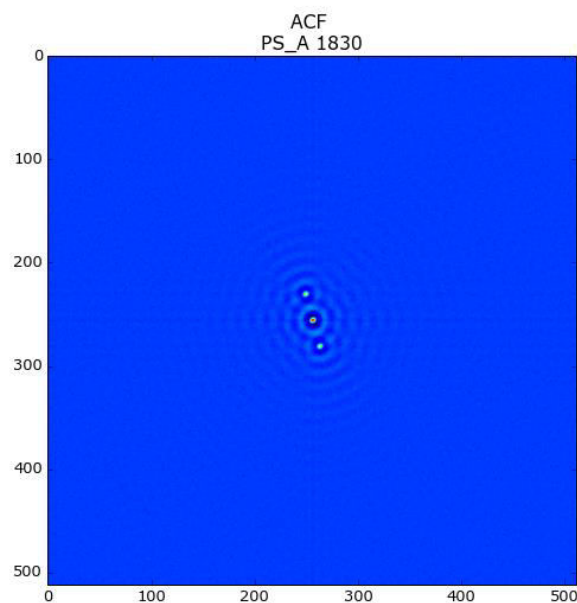


**Figure 4.** Autocorrelation function showing the central and both secondary peaks.

## 5. Quadrant determination

Several techniques can be applied to determine the real peak. "Shift-and-add" techniques used on the read-out noise corrected speckle frames will solve most of the wide and middle open pairs, depending not only in the separation but also in seeing conditions and difference in magnitude between components. Close pairs require more advanced techniques as bispectrum or, once that we are able to determine accurately the position and the difference in magnitude between both components, we can multiply each speckle frame by a function that changes monotonically in the direction from the primary to the secondary component resulting in a change in the magnitude difference between components as suggested by Walker (Walker et al.1978). All these techniques had being used in the past by different research teams but, up until now, a comparison between them had not been published.

## 6. Conclusions

Summarizing the preliminary results of our three campaigns, which had been completed using the OARMA speckle camera attached to the 2.6 m telescope of BAO we have to note the following:

a) More than four hundred double and multiple objects with the intention to obtain their relative positions and differential magnitudes has been observed during the last three observational campaigns.

b. The preliminary estimations are show that a separation limit between the binaries beyond 90 mas could be measured, and the objects as faint as 12 magnitudes could be able to solved in present observations.

The first scientific results of these observations we hope to present for publications in May-June 2018.

**Acknowledgement.** J. Gómez would like to thank all the BAO staff for their scientific support, and to D.A. Rastegaev, A.F. Maksimov, V.V. Dyachenko, E.V. Malogolovets and Yu.Yu. Balega, from SAO's speckle group. We have to express authors thanks to BAO's Director A. M. Mickaelian and Deputy director H. A. Harutyunyan for permanent interest to our observations.

## Reference

Horch, E.P.; Casetti-Dinescu, D.I., et al. 2017, A J., 153, 212  
Tokovinin, A.; Mason, B.D.; Hartkopf, W.I.; Mendez, R.A.; Horch, E.P., 2016, AJ., 151, 153

- Tamazian, V.S.; Docobo, J.A.; Balega, Y.Y.; Melikian, N.D.; Maximov, A.F.; Malogolovets, E.V. 2008, AJ., 136, 974
- Docobo, J.A.; Tamazian, V.S.; Balega, Y.Y.; Melikian, N.D. 2010, AJ., 140, 1078
- Maksimov, A.F.; Balega, Y.Y.; Dyachenko, V.V.; Malogolovets, E.V.; Rastegaev, D.A., Semernikov, E.A. 2009, Astrophs. Bu., 64, 296
- Hartkopf, W.I.; Mason, B.D.; Worley, C.E. 2001, AJ., 122, 3472 (see also <http://ad.usno.navy.mil/wds/orb6.html>)
- Pluzhnik, E.A. 2005, A&A, 431, 587
- Walker, R.L. 1978, BAAS, 10, 410